

On the Inhomogeneity of Low Nickel Loading Methanation Catalyst

Chang-Wei Hu,* Jie Yao,† Hua-Qing Yang,* Yu Chen,* and An-Min Tian*

*Department of Chemistry, Sichuan University, Chengdu, Sichuan 610064, People's Republic of China; and †Chemical Institute in Chengdu, Academy of China, Chengdu, Sichuan 610013, People's Republic of China

Received March 23, 1995; revised February 26, 1996; accepted September 30, 1996

Temperature-programmed reduction (TPR) and continuous stepwise reduction–methanation (CSR) have been used to identify and separate the active phases of Ni/Al₂O₃ catalyst. It is found that there are four hydrogen consumption peaks representing four nickel species on Al₂O₃; the peak temperatures for three of them are below 673 K when the reduction temperature does not exceed to 973 K. For the methanation of both CO and CO₂, three distinct active phases are discovered, the activation temperatures of which coincide with the peak temperatures of the first three TPR peaks, respectively. This indicates that different oxidized nickel species exist on Al₂O₃ prior to reduction and form different active phases for the methanation of both CO and CO₂ after reduction. The methanation activities on each phase for both CO and CO₂ in terms of CH₄ yield or initial methanation temperature and turnover number differ significantly. Each phase also exhibits different activity for CO and CO₂ methanation. It is suggested that the mechanism of methanation for CO or CO₂ on different phases may vary, and that the mechanism for CO and CO₂ on the same phase may also vary. CSR is convenient for separating different active phases for the methanation of both CO and CO₂ on Ni/Al₂O₃ catalyst. © 1997

Academic Press

INTRODUCTION

Low nickel loading Ni/Al₂O₃ catalyst was found to exhibit CO hydrogenation performance that differed from high loading ones, and two distinct methanation sites were found by temperature-programmed reaction of adsorbed CO (1–4). The two sites were assigned to Ni atoms bonding to other nickel atoms and Ni atoms interacting strongly with an oxide phase of the support (2) or assigned to Ni atoms formed from the reduction of crystalline NiO and NiAl₂O₄ (3, 4). The methanation activity of Ni/Al₂O₃ catalyst depended intimately on the surface chemical state of Ni, and different active phases formed from the reduction of different nickel species in the oxidated states (5). From the results of interrupted temperature-programmed reaction of adsorbed CO with isotope labeling, Glugla *et al.* (6) proposed that among the two sites, one was on Ni metal and the other was on the support. Zielinski (5) found that nickel oxides appeared in Ni/Al₂O₃ in two forms prior to

reduction, as “free” and “fixed” oxides, and formed large and small crystallites, respectively, when reduced. The difficulty of reduction of the supported catalysts was due to the chemical interaction of nickel oxide with the support. These results indicated that the active surface of Ni/Al₂O₃ was not homogeneous for methanation reaction. One may ask, what is the relationship between active phases and the reduction temperatures of the catalyst? Are there any differences between the performance of different active phases?

It was considered that the methanation of both CO and CO₂ proceeded by the same mechanism on Ni/SiO₂ and Ni/SiO₂–Al₂O₃ (8) and even on each type of the two distinct active sites on Ni/Al₂O₃ (9). However, CO₂ could be converted to CH₄ at lower temperature than that for CO on Ni/Al₂O₃ when each of them reacted solely with H₂ (10). The molecular structure of CO₂ differs greatly from that of CO, but they form the same product CH₄ when they react with H₂ over Ni-based catalyst. It will be valuable to understand the essence of these facts.

The scope of this investigation is to correlate the morphology before and after reduction and the catalytic performance, and to examine and separate the contribution of each active phase under reaction conditions. We also attempt to explore if there are differences between the catalytic activation of CO and CO₂ on each active phase of Ni/Al₂O₃.

EXPERIMENTAL

The catalyst was prepared by wet impregnation using a nickel nitrate solution. High purity γ -Al₂O₃ (Mg < 0.003%, Mn < 0.001%, Si < 0.01%, Fe < 0.003%, Cu < 0.0001%) with BET surface area about 140 m² and a particle size of 20–40 mesh was used as support. The support was degassed at room temperature before impregnation. The nickel concentration of the solution was controlled to make the final nickel content of the catalyst to be less than 10 mass%. The support was impregnated for 24 h and the excess solution was poured out to avoid nickel aggregation. Then the supported nickel nitrate was dried in a vacuum system and calcined at 673 K for 4 h in air flow. The final nickel

TABLE 1

The Percentage of Ni Exposed at Different Activation Temperature Based on H₂ Adsorption^a

Activation temperature (K)	535	573	673
Total exposed Ni ^b	2.26	13.27	23.28
Total Ni contained in the sample (%)	2.26	11.01	10.01
Amount of exposed Ni formed ^c	2.26	11.01	10.01
Total Ni contained in the sample (%)	2.26	11.01	10.01

^a The turnover number is calculated by the amount of exposed Ni formed at the activation temperature.

^b The total exposed Ni is calculated directly from H₂ adsorption.

^c The amount of exposed Ni formed at 535 K is also the total exposed Ni at 535 K. The amount of exposed Ni formed at 573 K is obtained by subtraction of the total exposed Ni formed at 535 K from the total exposed Ni at 573 K. The amount of exposed Ni formed at 673 K is obtained by subtraction of the total exposed Ni formed at 573 K from the total exposed Ni at 673 K.

content of the finished catalyst is 9.3 mass% as determined by atomic absorption spectroscopy.

The TPR experiment is similar to that described previously (5). A 0.095-g sample of catalyst was placed in a U-tube copper reactor. An electric furnace was used to heat the catalyst from room temperature to 973 K at 15 K/min, with 1:9 mixture of ultrapure H₂ and N₂ flowing over the catalyst at normal pressure at 40 ml/min. A thermal conductivity cell was used to detect the decrease of H₂ concentration.

The number of exposed surface Ni was determined by pulse chromatographic technique similar to that used by D. Duprez *et al.* (11). The catalyst was reduced at given temperature (535, 573, and 673 K, respectively) in H₂ (99.99%) flow for 2 h and then flashed by Ar (99.999%) flow at the reduction temperature for 1 h. The system was cooled to 280 K with Ar flow. A pulse of Ar + H₂ (10% H₂) mixture was injected to the reduced sample to saturation. The amount of chemisorbed H₂ (H_c) was determined from the peak heights of the unsaturated hydrogen,

$$H_c = N_c \left(nH_m - \sum H_i \right) / H_m,$$

where N_c is the number of moles of H₂ in a pulse, n the pulse number, H_m the peak height at saturation, and H_i the peak height of i th pulse. The number of exposed surface Ni was calculated by assuming $H/Ni = 1$ (12). The percentage of exposed surface Ni to the total Ni contained in the sample is given in Table 1.

The continuous stepwise reduction methanation measurement was carried out by putting 1 ml (0.3118 g) of catalyst on a frit to flow down into a 1.0-cm-diameter fixed-bed quartz reactor operated at atmospheric pressure. A mixture of H₂ + CO (or CO₂) was used both as activator for the catalyst and as reaction feed. The water formed in

the methanation reaction was trapped by an ice trap connected to the reactor. A gas chromatographic system equipped with a microcomputer was used to analyze the effluent gas from the reactor. The temperature was elevated stepwise to 673 K using a tube electric furnace, the detail of temperature control will be described under Results and Discussion to avoid duplication. CH₄ yield is defined as $y\% = \frac{\text{the amount of CO}_x \text{ converted to CH}_4}{\text{the amount of CO}_x \text{ in the feed}}$, where $x = 1$ for CO and 2 for CO₂.

RESULTS AND DISCUSSION

TPR

Figure 1 shows the TPR curves for the catalyst and spectroscopically pure NiO and Ni₂O₃ powders. There is only a single H₂ consumption peak for both pure NiO and Ni₂O₃ powders, at 678 and 611 K, respectively. However, for the catalyst sample, four hydrogen consumption peaks appear, which is in accordance with TPR curves reported previously (13). The peak temperatures for the first two peaks (510 and 580 K) are lower than that of Ni₂O₃ (611 K). The initial point of the first peak (about 470 K) is much lower than that for Ni₂O₃ (530 K), whereas the final point of the second peak

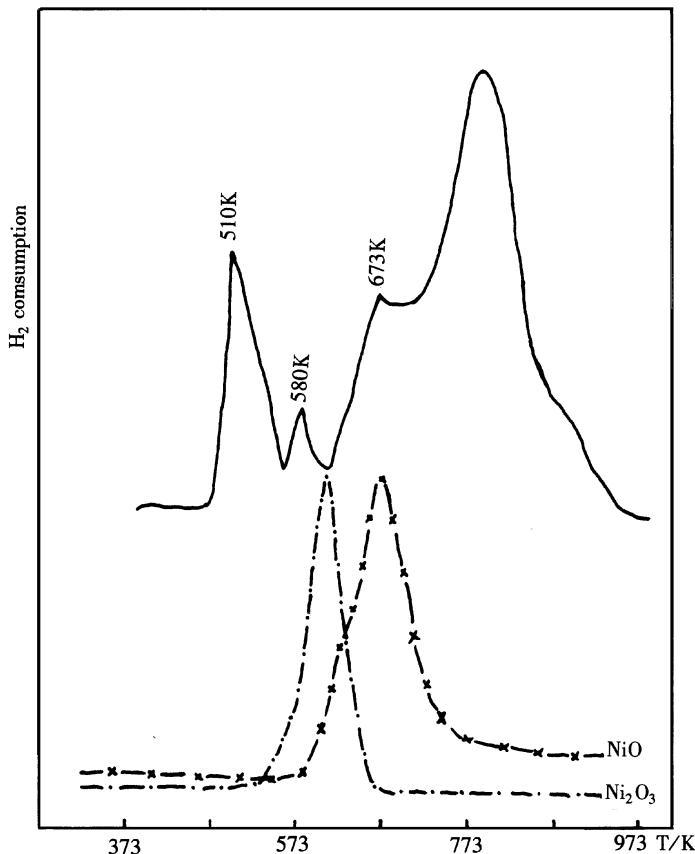


FIG. 1. The TPR curve of the catalyst.

(about 610 K) is near the peak temperature of Ni₂O₃. The third and fourth peaks overlap, and the third one has almost the same peak temperature as NiO powder (678 K); however, the peak temperature of the fourth peak (about 800 K) is even higher than the final point for NiO (about 770 K). These data reveal that the reduction of both NiO and Ni₂O₃ powders occurs in only one step. The four TPR peaks of the catalyst may represent four chemically different oxidized nickel species existing on Al₂O₃ prior to reduction. It was previously suggested that the low temperature TPR peaks of Ni/Al₂O₃ system originated from the total reduction of crystalline NiO or Ni₂O₃, highly dispersed NiO or Ni₂O₃ monolayers, and/or other dispersed nickel species (5). Thus the four TPR peaks on the present catalyst are the evidence of the existence of highly dispersed nickel species (the first two peaks), crystalline Ni₂O₃ (the second peak), crystalline NiO (the third peak), and the so-called "fixed" nickel species (the fourth peak) on Al₂O₃.

CSRM

Now that the feed for the methanation over Ni/Al₂O₃ is also the activator for the catalyst, it is possible to activate the catalyst under reaction conditions. In CSRM measurement, the catalyst is activated by heating to about 473 K and held in H₂ flowing at 20 ml/min. After a constant temperature is attained, CO or CO₂ is added to provide a H₂/CO (or CO₂) mixture and the flow rates of H₂ and CO (or CO₂) are adjusted to make CO/H₂ = 1/3 (CO₂/H₂ = 1/4, i.e., under stoichiometric proportion) and GHSV = 1260 h⁻¹; the effluent is analyzed simultaneously. No CH₄ is detected at 473 K. Then the composition and flow rate of the feed are maintained and the temperature is elevated stepwise by steps of about 10 K and maintained constant again with simultaneous analysis of the effluent. CH₄ is not detected until 530 K, and at 535 K the amount of CH₄ formed initially increases with increasing time, reaches a maximum, and finally remains constant for both CO/H₂ and CO₂/H₂. It indicates that the first active phase for the methanation of both CO and CO₂ is activated at about 535 K; it will be named phase C. The increase of CH₄ yield with time indicates the activation process of the active phase and the final constant CH₄ yield indicates the ending of the activation. After that the system is cooled stepwise by steps of about 10 K to investigate the temperature dependence of methanation activity. When the temperature is lower than 510 K for CO/H₂ and 520 K for CO₂/H₂, CH₄ disappears. It indicates that phase C starts to show methanation activity for CO at about 510 K and for CO₂ at about 520 K. The system is then heated and cooled again in the same manner. Two phenomena are indicative for the formation of new active phase. If there is an active phase formed at a temperature, an increase in CH₄ yield within time at this temperature will be observed at first, and gradually a maximum value will be reached and become constant at this temperature. The CH₄ yield at the

nearest low temperature on cooling will be higher than that obtained at the same temperature on heating. The highest activation temperature is 673 K in the present study to avoid sintering. Two other phases activated at 573 and 673 K were discovered and named phase B and phase A, respectively. It is interesting that the activation temperatures for phases C, B, and A are in good agreement with the peak temperatures of the first three TPR peaks, respectively. It is possible that phases C, B, and A are formed from the reduction of the nickel species which give the first three TPR peaks. The name of the active phases are given in accordance with those given by K. B. Kester *et al.* (2, 9) according to their methanation activity to facilitate comparison.

Inhomogeneity of the Active Phases in the Methanation of CO

Figure 2 shows the changes of the total CH₄ yield and the contribution of each active phase to methanation, with increasing temperature. The contribution of phase C is acquired directly, whereas that of phase B is acquired by a subtraction of the curve obtained when the catalyst is activated at 535 K from the curve obtained when the catalyst is activated at 573 K. As phase A exhibits much greater activity than phases B and C, CO could be almost completely converted to CH₄ at much lower temperature than that at which phases B and C start to show activity. Then the curve obtained when the catalyst is activated at 673 K represents directly the contribution of phase A, as shown in Fig. 2. Phase B starts to show methanation activity at almost the same temperature as that of phase C, but the contribution of phase B is less than that of phase C. It is obvious that the relative order of activity, in term of CH₄ yield or initial methanation temperature, is phase A > phase C > phase B over the temperature range tested. Figure 3 shows the specific methanation activity in terms of turnover number (number of moles of CH₄ converted per mole of exposed surface Ni per hour). It is clear that the surface Ni in phase C is much

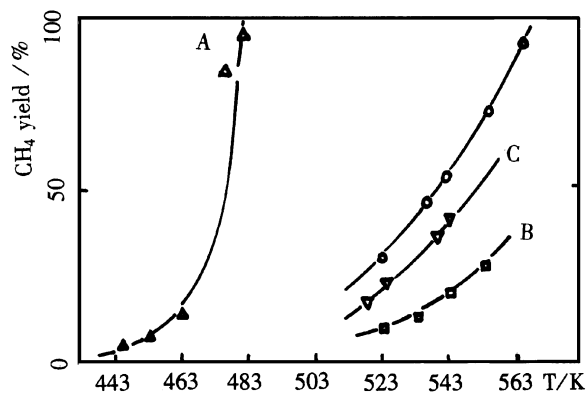


FIG. 2. CO methanation activity in terms of CH₄ yield. Δ , Total after activated at 673 K (phase A), \circ , Total after activated at 573 K. \square , Contribution of phase B. ∇ , Total after activated at 535 K (phase C).

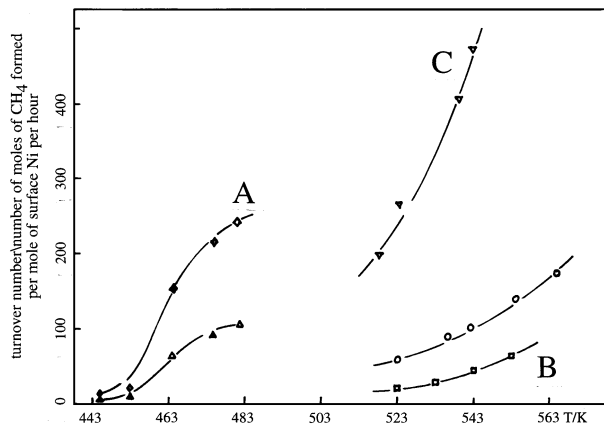


FIG. 3. CO methanation activity in terms of turnover number based on H_2 adsorption. Δ , Total after activated at 673 K. \diamond , Contribution of phase A. \circ , Total after activated at 575 K. \square , Contribution of phase B. ∇ , Total after activated at 533 K (phase C).

more active than that in phase B over the same temperature range. The temperature needed for a given turnover number (e.g., 200) over phase A is much lower than those over phases B and C, respectively; thus the surface Ni in phase A is more active than those in phases B and C. The initial methanation temperatures and the apparent activation energies obtained from the Arrhenius plots of the space time yield of CH_4 vs temperature is shown in Table 2. The initial methanation temperatures for phases A and B are a little lower and near, respectively, the methane peak temperatures obtained by temperature-programmed reaction of adsorbed CO on Ni/Al_2O_3 with similar nickel loading (10.5 wt%) (9), but the apparent activation energies are different from these found in the literature (9). It is possible that phases A and B named in present study are similar

TABLE 2

The Initial Methanation Temperature and the Apparent Activation Energy

	Active phase		
	C	B	A
Activation temperature (K)	535	573	673
Initial temperature for CO methanation (K)	510	510 (498) ^a	440 (445) ^a
App. Act. Eng. for CO methanation ($kJ\ mol^{-1}$)	101.0	56.5 (145) ^b	83.1 (51) ^b
Initial temperature for CO_2 methanation (K)	520 (650) ^a	470 (498) ^a	440 (445) ^a
App. Act. Eng. for CO_2 methanation ($kJ\ mol^{-1}$)	53.6	101.4	178.8

^a The values in the parentheses are the methane peak temperature in temperature-programmed reaction of adsorbed CO or CO_2 reported previously (9).

^b The values in the parentheses are the activation energies obtained by temperature-programmed reaction of adsorbed CO (2).

to those reported previously (2, 9). The difference in apparent activation energies might be caused by the use of two different techniques. Since the present method is carried out under steady reaction conditions, the values obtained hereby might approach the real ones. These data show that each active phase behaves differently in the methanation of CO, although the products are the same.

Inhomogeneity of the Active Phases in CO_2 Methanation

The CO_2 methanation activity on the catalyst is similar to CO methanation, as shown in Figs. 2 and 4. However, it should be noted that the relative order of activity in terms of CH_4 yield and initial methanation temperature is phase A > phase B > phase C, which is different from CO methanation. Especially noticeable is that phase B starts to exhibit detectable activity at a much lower temperature than phase C. The relative order of specific activity expressed by turnover number for phases A and B is the same as that expressed by CH_4 yield, though the difference is not significant, as shown in Fig. 5. However, the surface Ni atom in phase C becomes the most active in terms of turnover number. The initial methanation temperature and the apparent activation energies on each phase for CO_2 are listed in Table 2. The values of apparent activation energies for CO_2 methanation on phase C (53.6) and phase B (101.4) are close to those summarized by G. D. Weatherbee and C. H. Bartholomew (54.3, 54.8, 94, 105.8 kJ/mol) (14). It is evident that each phase behaves differently in the methanation of CO_2 . Moreover, no detectable CO is observed in the whole process of activity measurement.

Inhomogeneity on Each Active Phase between the Methanation of CO and CO_2

As shown in Figs. 2–5 and Table 2, the phase which is active for the methanation of CO acts also as active phase

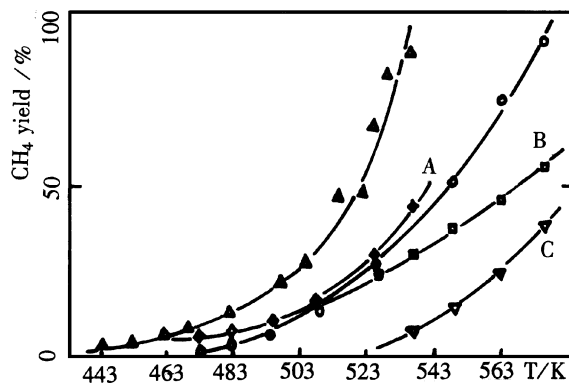


FIG. 4. CO_2 methanation activity in terms of CH_4 yield. Δ , Total after activated at 673 K. \diamond , Contribution of phase A. \circ , Total after activated at 575 K. \square , Contribution of phase B. ∇ , Total after activated at 535 K (phase C).

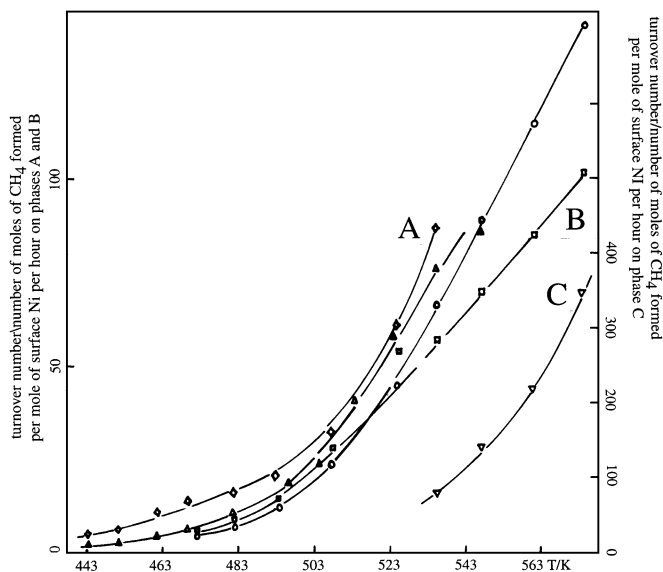


FIG. 5. CO₂ methanation activity in terms of turnover number based on H₂ adsorption. Δ , Total after activated at 673 K. \diamond , Contribution of phase A. \circ , Total after activated at 573 K. \square , Contribution of phase B. ∇ , Total after activated at 535 K (phase C).

for the methanation of CO₂. Nevertheless, each phase behaves differently. On phase C, the activity both in terms of CH₄ yield and of turnover number for CO methanation is higher than that for CO₂ over the whole temperature range tested, and the apparent activation energy is nearly two times greater than that for CO₂. Phase B starts to show CO₂ methanation activity at about 470 K and CO methanation activity at about 510 K, moreover both the CH₄ yield and turnover number for CO₂ methanation are greater than those for CO over the whole temperature range tested. The apparent activation energy for CO₂ methanation is nearly two times greater than that for CO. Although phase A starts to show methanation activity for both CO and CO₂ at almost the same temperature, the CH₄ yield and turnover number for CO methanation are greater than those for CO₂, and the apparent activation energy for CO₂ methanation is two times greater than that for CO. It is obvious that phases A and C are more active for CO methanation than for CO₂, while phase B is more active for CO₂ methanation than for CO under stoichiometric ratios of H₂/CO and H₂/CO₂.

For the methanation of CO, we find three active phases; this is one more than was observed by K. B. Kester *et al.* (2, 9). There are two possible reasons for this. First, because phases B and C start to exhibit methanation activity at the same temperature, the transient technique, temperature-programmed reaction of adsorbed CO, may not be capable of separating their contributions. Second, it is possible that phase C does not adsorb CO in the absence of hydrogen and/or at low temperature. It is the CO adsorbed at high temperature or co-adsorbed CO and H₂ which causes the hydrogenation, and then the temperature-programmed

reaction of CO adsorbed at 298 K could not identify it. For the methanation of CO₂, three active phases are observed. This is in accordance with the result of K. B. Kester *et al.* (9). On phases A and B, the initial methanation temperatures are a little lower than the CH₄ peak temperatures in temperature-programmed reaction of adsorbed CO₂, respectively, which is in agreement with the findings in the literature (9). On phase C, the initial methanation temperature is much lower than the peak temperature in temperature-programmed reaction of adsorbed CO₂, but it should be noted that the methane peak in temperature-programmed reaction of adsorbed CO₂ is a broad one; thus the peak temperature ought to be much higher than the initial temperature. Then phase C, in the present work, is also in accordance with the findings in the literature (9).

Phase A is assigned to Ni atoms bonding to other nickel atoms, i.e., nickel crystallites (2, 4, 6, 9). The data in the present work support this assignment. The TPR of the sample also provides new information for this assignment. Phase A is originated from the reduction of NiO crystallites.

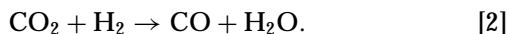
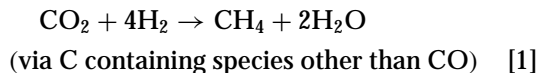
Concerning the origin of phase B, P. G. Glugla *et al.* (6, 15) proposed that it was on the support Al₂O₃. Y. J. Huang *et al.* (4) assigned it to nonreducible NiAl₂O₄-like species. The TPR and CSR results suggest that this phase might form from the reduction of Ni₂O₃ species or highly dispersed nickel species which could be reduced at 573 K, because it exhibits no methanation activity when it is reduced below 573 K.

Phase C has been observed by K. B. Kester *et al.* (9) using temperature-programmed reaction of adsorbed CO₂, but little information about this phase has been proposed. The TPR and CSR results reveal that phase C is originated from the reduction of highly dispersed surface nickel species which could be reduced at 535 K. It acts as active phase for the methanation of both CO and CO₂.

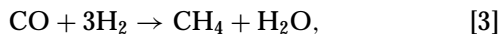
The agreement of initial methanation temperature of phase A, B, and C in present study with those observed previously (9) from temperature-programmed reaction of adsorbed CO₂ may support the assignment of the TPR results. The nickel species reduced at low temperature do not experience further reduction at higher temperature when the other nickel species are reduced.

The methanation of CO₂ on nickel-based catalyst is considered to proceed by the same mechanism as that of CO (8, 9). M. Araki *et al.* suggested that the first step of CO₂ methanation is the reduction of CO₂ to CO, and this step was considered to be faster than CO methanation (16). R. Maatman *et al.* proposed a slow two-step mechanism, i.e., the dissociation of H₂ and CO₂ and either of the two steps could be rate-determining (17). T. V. Herwijnen *et al.* suggested that the adsorption of CO₂ on the clean surface is rate-determining (18). In comparing the methanation rates between CO₂ and CO, it is well known that on nickel and nickel alloy catalysts, the CO₂ methanation activities

are smaller than CO methanation activity (19, 20). Previous studies show that CO₂ could be converted to methane at lower temperature than that for CO on Ni/Al₂O₃ with 6 wt% nickel loading (10) and on Rh supported on ZrO₂, Al₂O₃, SiO₂, and MgO (21). T. Iizuka *et al.* discovered that on Ni-La₂O₃-Ru/SiO₂ and Ru/SiO₂ the rate of CO₂ methanation is greater than that for CO (20, 22). The apparent activation energy for CO₂ is less than that for CO on composite catalysts containing Ni (22). G. D. Weatherbee and C. H. Bartholomew (14, 23) discovered that on Ni/SiO₂ the CH₄ turnover number for CO₂ methanation is slightly higher at 500 K, the same at 525 K, and slightly lower at 550 K than for CO methanation. They also proposed a mechanism which proceeded via CO₂ dissociation to CO and CO hydrogenation. These results seem to be a little contradictory. The CSRM data reveal that on phases A and C, the CO₂ methanation activity is indeed much lower than that for CO, but the temperature dependence of CH₄ yield for CO₂ hydrogenation differs remarkably from that for CO hydrogenation. While on phase B, not only does the temperature dependence vary but so does the initial methanation temperature. If the first step of CO₂ hydrogenation is to be converted to CO, and this step is a fast step, the tendency of temperature dependence of CH₄ yield should be similar, and the initial methanation temperature should not be so obviously lower than that for CO. The disagreement or even contrary opinions by different authors on the mechanism of CO₂ methanation might come from two origins. They are the heterogeneity, as proposed by T. V. Herwijnen *et al.* (18) in the active phases on the catalysts, and the complexity of possible reactions of the reactants. Different active phases existing on the catalyst are scarcely studied separately under reaction conditions. The distribution of different active phases, the contribution of which differs from one to another, may change on different catalysts studied by different researchers; then the total performance of the catalysts originated from the overlaps of different active phases may vary. Concerning the possible reactions of the reactants, there are at least two different reaction paths which compete; i.e.,



After reaction [2] occurs, the probability of the other two reactions will rise; i.e.,



and the reverse reaction of [2]. In this case, any changes in the concentration of CO₂ or H₂ usually used in kinetics studies will probably change the variation of Gibbs free energy (ΔG) of a certain reaction and then change the possibility

for the reaction to occur. In fact, the variation of CO₂/H₂ ratio could cause a change in ΔG as large as 10 kJ/mol. Reaction [2] is thermodynamically unfavorable at low temperature, while reaction [1] is unfavorable at high temperature. Under this consideration, the variation in ΔG would result in the complexity of the system. In fact, the results of G. D. Weatherbee and C. H. Bartholomew (14) showed that the kinetic behavior of the system when H₂/CO₂ > 4/1 differed from that when H₂/CO₂ < 4/1. It should be noted that the use of CSRM could not avoid the thermodynamic complexity of the system. More detailed information from each active phase may give more acceptable explanations. What is certain is that Ni/Al₂O₃ with low nickel loading exhibits remarkably different activity in the methanation of CO or CO₂ when it is reduced at different temperatures. The catalyst also shows different methanation activity for CO and CO₂ when it is reduced at the same temperature under the conditions tested in present work.

CONCLUSION

(1) CSRM method is efficient for the separation of different active phases on Ni/Al₂O₃ catalysts under steady-state reaction conditions.

(2) Three distinct active phases for the methanation of both CO and CO₂ exist on Ni/Al₂O₃ with low nickel loading. They originate from the reduction of different nickel species which could be reduced at different temperatures. The relative activity order in terms of CH₄ yield and turnover number for the methanation of CO is phase A > phase C > phase B. The relative activity order in term of CH₄ yield for CO₂ methanation is phase A > phase B > phase C, and in term of turnover number is phase C > phase A > phase B. Phases A and C exhibit higher methanation activity for CO than for CO₂, while phase B shows higher activity for CO₂ than for CO.

ACKNOWLEDGMENT

We are grateful to the National Natural Science Foundation of China for the support of this work.

REFERENCES

1. Bartholomew, C. H., Pannell, R. B., and Butler J. L., *J. Catal.* **65**, 335 (1980).
2. Kester, K. B., and Falconer, J. L., *J. Catal.* **89**, 380 (1984).
3. Huang, Y. J., and Schwarz, J. A., *Appl. Catal.* **32**, 45 (1987).
4. Huang, Y. J., Schwarz, J. A., Diehl, J. R., and Baltrus, J. P., *Appl. Catal.* **36**, 163 (1988).
5. Hu, C. W., Wang, W. Z., Pan, X., Xu, G. Y., and Chen, Y., *J. Natural Gas Chem.* **3**(2), 194 (1994).
6. Glugla, P. G., Bailey, K. M., and Falconer, J. L., *J. Phys. Chem.* **92**, 4474 (1988).
7. Zielinski, J., *J. Catal.* **76**, 157 (1982).
8. Campell, T. K., and Falconer, J. L., *Appl. Catal.* **50**, 189 (1989).

9. Kester, K. B., Zagli, A. E., and Falconer, J. L., *Appl. Catal.* **22**, 311 (1986).
10. Hu, C. W., Peng, X. M., Wang, W. Z., Chen, Y., and Tian, A. M., *Chem. Res. Appl. (Huaxue Yanjiu Yu Yingyong)* **6**(3), 54 (1994).
11. Duprez, D., Mendez, M., and Dalmon, J. A., *Appl. Catal.* **21**, 1 (1986).
12. Bartholomew, C. H., and Pannell, R. B., *J. Catal.* **65**, 390 (1980).
13. Tang, X. S., Huang, S. M., and Jin, S. S., *Chem. J. Chin. Univ. (Gaodeng Xuexiao Huaxue Xuebao)* **12**(4), 514 (1991).
14. Weatherbee, G. D., and Bartholomew, C. H., *J. Catal.* **77**, 460 (1982).
15. Glugla, P. G., Bailey, K. M., and Falconer, J. L., *J. Catal.* **115**, 24 (1989).
16. Araki, M., and Ponec, V., *J. Catal.* **44**, 439 (1976).
17. Maatman, R., and Hiemstra, S., *J. Catal.* **62**, 349 (1980).
18. Herwijnen, T. V., Doesburg, H. V., and Dejong, W. A., *J. Catal.* **28**, 135 (1973).
19. Luengo, C. A., Cabrera, A. L., Mackay, H. B., and Maple, M. B., *J. Catal.* **47**, 1 (1977).
20. Inui, T., and Funabiki, M., *Chem. Lett.*, 251 (1978).
21. Iizuka, T., Tanaka, Y., and Tanabe, K., *J. Catal.* **76**, 1 (1982).
22. Inui, T., Funabiki, M., Suehiro, M., and Sezume, T., *J. Chem. Soc. Faraday Trans. 1* **75**(4), 787 (1979).
23. Weatherbee, G. B., and Bartholomew, C. H., *J. Catal.* **68**, 67 (1981).